Int. J. Heat Mass Transfer. Vol. 28, No. 3, pp. 653–662, 1985
Printed in Great Britain

0017 9310/85 $3.00 + 0.00
Pergamon Press Ltd.

Numerical prediction of an asymmetrical heated plane jet with a second-moment turbulence closure

I. DEKEYSER

U.E.R. Institut de Mécanique Statistique de la Turbulence, Université d'Aix-Marseille II, 12, Avenue Général Leclerc, 13003 Marseille, France

(*Received* 23 *May* 1984)

Abstract—The paper deals with the application of a second-moment turbulence closure to the calculation of an asymmetrical heated plane jet. Different closure models for the triple velocity and velocity–temperature correlations have been tested. The numerical solutions obtained with a modified Patankar–Spalding finite-difference method, the most important modification being the staggering of the location of nodes for the turbulence variables to mean-field nodes, are compared to the experimental data.

1. INTRODUCTION

NUMERICAL prediction of heated turbulent shear flows of engineering interest have seen extensive progress over the past decade. Second-moment turbulence closures which originated with the work of Rotta [1] have been extensively used. In these schemes the second-moment correlations representing the turbulent transport of momentum, heat or any other scalar are themselves subjects of a set of approximated transport equations which are solved simultaneously with those for the mean fields. This kind of approach may be contrasted with the usual phenomenological treatment which, by analogy with molecular transport models, are based on an effective turbulent viscosity and effective turbulent Prandtl number. The reason for preferring a second-moment model is that the turbulence interactions which generate the turbulent stresses and heat fluxes can be treated exactly. Moreover Boussinesq closure is inappropriate for flows presenting counter-gradient zones.

The applications of second-moment turbulence closure models have been largely limited to moment transport processes. The studies of heat transport phenomena have not been extensively considered. It must be said, however, that experimental documentation of detailed turbulence statistics for heat transport phenomena is still not plentiful.

The present paper presents the application of a second-moment turbulence closure model to the calculation of a heated asymmetrical plane jet, the temperature being considered a passive contaminant. Section 2 provides a presentation of the mathematical model and section 3 the method of numerical solution. Comparison between model simulation and experimental data (Dekeyser [2]) is provided in section 4, while concluding remarks are presented in section 5.

2. THE PHYSICAL AND MATHEMATICAL MODEL

The instantaneous Navier–Stokes equations for low-speed flow of fluid with uniform density may be written, with conventional time averaging (Favre [3]), for a statistically stationary flow

$$\frac{\partial U_i}{\partial x_i} = 0 \tag{1}$$

$$U_j\frac{\partial U_i}{\partial x_j} = -\frac{1}{\rho}\frac{\partial P}{\partial x_i} + \nu\frac{\partial^2 U_i}{\partial x_i \partial x_j} - \frac{\partial \overline{u_i u_j}}{\partial x_j}. \tag{2}$$

Similarly an energy equation can be written as

$$U_j\frac{\partial \Theta}{\partial x_j} = \alpha\frac{\partial^2 \Theta}{\partial x_j \partial x_j} - \frac{\partial \overline{u_j\theta}}{\partial x_j} \tag{3}$$

The numerical solution of the above set of equations requires the introduction of additional expressions, or additional transport equations for $\overline{u_i u_j}$ and for $\overline{u_j\theta}$. The heated asymmetric plane jet presents [2] simultaneously two counter-gradient diffusion zones, one for the dynamical field, the other for the thermal field. Also, effective viscosity and diffusivity concepts cannot be retained for this type of flow. For this reason turbulent transport equations for $\overline{u_i u_j}$ and $\overline{u_j\theta}$ have been introduced

$$\begin{aligned} U_k\frac{\partial \overline{u_i u_j}}{\partial x_k} = &-\left(\overline{u_i u_k}\frac{\partial U_j}{\partial x_k} + \overline{u_j u_k}\frac{\partial U_i}{\partial x_k}\right) \\ &-2\nu\overline{\frac{\partial u_i}{\partial x_k}\frac{\partial u_j}{\partial x_k}} - \frac{\partial}{\partial x_k}\left(\overline{u_i u_j u_k}\right. \\ &\left.-\nu\frac{\partial \overline{u_i u_j}}{\partial x_k} + \overline{\frac{p}{\rho}(\delta_{kj}u_i + \delta_{ki}u_j)}\right) \\ &+\overline{\frac{p}{\rho}\left(\frac{\partial u_i}{\partial x_j} + \frac{\partial u_j}{\partial x_i}\right)} \end{aligned} \tag{4}$$

$$\begin{aligned} U_k\frac{\partial \overline{u_j\theta}}{\partial x_k} = &-\left(\overline{u_j u_k}\frac{\partial \Theta}{\partial x_k} + \overline{u_k\theta}\frac{\partial U_j}{\partial x_k}\right) \\ &-(\alpha+\nu)\overline{\frac{\partial \theta}{\partial x_k}\frac{\partial u_j}{\partial x_k}} - \frac{\partial}{\partial x_k}\left(\overline{u_j u_k \theta}\right. \\ &\left.-\alpha\overline{u_j\frac{\partial \theta}{\partial x_k}} - \nu\overline{\theta\frac{\partial u_j}{\partial x_k}} + \overline{\frac{p\theta}{\rho}}\delta_{jk}\right) + \overline{\frac{p}{\rho}\frac{\partial \theta}{\partial x_j}}. \end{aligned} \tag{5}$$

NOMENCLATURE

d width of the exit slot
k turbulent kinetic energy
l_{u_1} velocity length scale
l_θ, l_{θ_i} temperature length scales
P mean static pressure
p fluctuation of static pressure about mean value
R ratio of temperature and velocity dissipation time scales
U_i mean component of velocity in direction x_i
U_m maximum change in velocity across the flow
u_i fluctuation of x_i velocity component about mean value
x_i Cartesian coordinates.

Greek symbols
α thermal diffusivity
ε kinematic dissipation rate of kinetic energy
ε_θ dissipation rate of $\overline{\theta^2}/2$
$\eta_\xi = \dfrac{x_2 - x_{2\Xi}}{l_\xi}$ similarity variable for velocity field ($\xi = u_1, \Xi = U_m$) and for temperature field ($\xi = \theta, \Xi = \Delta\Theta_m$)
Θ mean temperature
$\Delta\Theta_m$ maximum variation of Θ across the flow
θ fluctuations in temperature about mean value
ν kinematic viscosity
ρ density.

Subscripts
e moving edge value
i stagnant edge value
0 slot exit value.

Superscripts
$\bar{}$ mean value
r.m.s. value.

Equations (4) and (5) are not immediately employable to find $\overline{u_iu_j}$ and $\overline{u_j\theta}$ since their right-hand sides contain still further unknowns. In a second-moment closure these unknown correlations must be approximated in terms of mean field distributions of velocity and temperature, the turbulent stress and heat fluxes, and a number of characteristic time scales (usually one, k/ε) to characterize the rate of which the various turbulence interactions proceed.

The closure proposals adapted in this study have in most respects appeared elsewhere in the literature and so only a brief presentation will be provided. The kinematic Reynolds stresses $\overline{u_iu_j}$ are obtained from the following set of transport equations:

$$U_k\frac{\partial\overline{u_iu_j}}{\partial x_k} = P_{ij} + \phi_{ij} - \varepsilon_{ij} + D(\overline{u_iu_j}) \tag{6}$$

where the four terms appearing on the RHS of equation (6) denote respectively: stress creation due to mean shear; redistributive action of the pressure-strain correlation; direct dissipation by viscous action and diffusive transport.

In mathematical form the pressure–strain correlation is approximated as

$$\phi_{ij} = \overline{\frac{p}{\rho}\left(\frac{\partial u_i}{\partial x_j} + \frac{\partial u_j}{\partial x_i}\right)} = \phi_{ij}^{(1)} + \phi_{ij}^{(2)} \tag{7}$$

where

$$\phi_{ij}^{(1)} = -c_{s_1}\frac{\varepsilon}{k}(\overline{u_iu_j} - \tfrac{2}{3}\delta_{ij}k) \tag{8}$$

and, following Naot *et al.* [4]

$$\phi_{ij}^{(2)} = -c_{s_2}(P_{ij} - \tfrac{2}{3}\delta_{ij}P) \tag{9}$$

with

$$P_{ij} = -\left(\overline{u_iu_k}\frac{\partial U_j}{\partial x_k} + \overline{u_ju_k}\frac{\partial U_i}{\partial x_k}\right), P = \tfrac{1}{2}P_{kk}. \tag{10}$$

The expression of ϕ_{ij} contains two coefficients c_{s_1} and c_{s_2} that are assigned constant values respectively 1.8 and 0.6 as adopted by Gibson and Launder [5] and Gibson and Rodi [6].

Following Rotta [1], Hanjalic and Launder [7] and nearly all subsequent workers we take

$$\varepsilon_{ij} = 2\nu\overline{\frac{\partial u_i}{\partial x_k}\frac{\partial u_j}{\partial x_k}} = \tfrac{2}{3}\delta_{ij}\varepsilon \tag{11}$$

where ε is the dissipation rate of kinematic energy.

Two models have been adopted for the diffusive transport of stress $D(\overline{u_iu_j})$ which at high turbulent Reynolds number with the hypothesis

$$\overline{\frac{pu_i}{\rho}} = 0$$

reduced to

$$D(\overline{u_iu_j}) = -\frac{\partial}{\partial x_k}(\overline{u_iu_ju_k})$$

—the simpler version proposed by Daly and Harlow [8]

$$D(\overline{u_iu_j}) = \frac{\partial}{\partial x_k}\left(c_s'\frac{k}{\varepsilon}\overline{u_ku_m}\frac{\partial u_iu_j}{\partial x_m}\right), \text{model } R_{D_1} \tag{12}$$

—the version proposed in [7]

$$D(\overline{u_i u_j}) = \frac{\partial}{\partial x_k}\left[c_s \frac{k}{\varepsilon}\left(\overline{u_k u_m}\frac{\partial \overline{u_i u_j}}{\partial x_m} + \overline{u_i u_m}\frac{\partial \overline{u_j u_k}}{\partial x_m} + \overline{u_j u_m}\frac{\partial \overline{u_i u_k}}{\partial x_m}\right)\right], \text{ model } R_{D_2}. \quad (13)$$

The two coefficients c_s' and c_s are assumed to be constants taking values obtained by numerical optimisation 0.22 [9] and 0.11 [7] respectively.

The closure of the model for calculating the dynamical field is completed through the following equation for the turbulence energy dissipation rate ε proposed by Launder *et al.* [10]

$$U_k \frac{\partial \varepsilon}{\partial x_k} = c_{\varepsilon_1}\frac{\varepsilon}{k}\overline{u_i u_j}\frac{\partial U_i}{\partial x_i} - c_{\varepsilon_2}\frac{\varepsilon^2}{k} + c_\varepsilon \frac{\partial}{\partial x_k}\left(\frac{k}{\varepsilon}\overline{u_k u_l}\frac{\partial \varepsilon}{\partial x_l}\right). \quad (14)$$

The three coefficients c_ε, c_{ε_1} and c_{ε_2} are assumed to be constants taking the values recommended by Launder and Morse [11] respectively 0.18, 1.45 and 1.90.

At high turbulent Reynolds and Peclet numbers, the terms in equation (5) containing the molecular transport coefficients are negligible. For flows, like the asymmetrical heated plane jet, with Prandtl numbers of order of unity their omission is entirely admissible. In these conditions, the turbulent heat fluxes are obtained from the following set of transport equations

$$U_k \frac{\partial \overline{u_j\theta}}{\partial x_k} = P_{j\theta} + \phi_{j\theta} + D(\overline{u_j\theta}) \quad (15)$$

the three terms appearing on the RHS of equation (15) denote respectively: the generative action of mean temperature and velocity gradients, which requires no approximation, the action of the pressure–temperature gradient correlation and diffusive transport.

For shear flows the pressure–temperature gradient correlation is by far the most crucial term to approximate. There are basically two different types of processes to be represented, one arising from purely turbulence interactions denoted $\phi_{j\theta}^{(1)}$ and a second one denoted $\phi_{j\theta}^{(2)}$ due to the presence of the mean strain [12]. Thus symbolically

$$\phi_{j\theta} = \overline{\frac{p}{\rho}\frac{\partial \theta}{\partial x_j}} = \phi_{j\theta}^{(1)} + \phi_{j\theta}^{(2)}. \quad (16)$$

Two models have been retained for the turbulence contribution—the simpler form suggested by Monin [13] and adopted by nearly all subsequent workers

$$\phi_{j\theta}^{(1)} = -C_{\theta_1}\frac{\varepsilon}{k}\overline{u_j\theta}, \text{ models } R_{T_1}, R_{T_2}, R_{T_4} \quad (17)$$

—the version proposed by Lumley and Khajeh-Nouri [14]

$$\phi_{j\theta}^{(1)} = -c_{\theta_1}\frac{\varepsilon}{k}\overline{u_j\theta} - c_{\theta_1}'\frac{\varepsilon}{k}\left(\frac{\overline{u_j u_l}}{k} - \frac{2}{3}\delta_{jl}\right)\overline{u_l\theta}, \text{ model } R_{T_3}. \quad (18)$$

In ref. [12] it was suggested that the most appropriate time scale with which to characterize this process would be $(k\overline{\theta^2}/\varepsilon\hat{\varepsilon}_\theta)^{1/2}$ where $\hat{\varepsilon}_\theta$ is the dissipation rate of $\overline{\theta^2}$. Since we do not employ a transport equation for $\hat{\varepsilon}_\theta$ we have adopted the scalar time scale of the turbulent velocity field k/ε.

The mean strain contribution $\phi_{j\theta}^{(2)}$ has been neglected in many closure schemes. We have considered here two models which have been in common use

—the quasi-isotropic model [15]

$$\phi_{j\theta}^{(2)} = 0.8\overline{u_k\theta}\frac{\partial U_j}{\partial x_k} - 0.2\overline{u_k\theta}\frac{\partial U_k}{\partial x_j}, \text{ model } R_{T_3} \quad (19)$$

—the destruction of production hypothesis

$$\phi_{j\theta}^{(2)} = c_{\theta_2}\overline{u_k\theta}\frac{\partial U_j}{\partial x_k}, \text{ models } R_{T_1}, R_{T_2}, R_{T_4}. \quad (20)$$

In the limit of vanishing small anisotropy, equation (19) may be shown to be exactly correct. For the highly sheared flows however it provides following [16] a less satisfactory approximation than equation (20). Therefore most of the calculated results presented in this paper are obtained with the set of equations (17) and (20), the coefficients c_{θ_1} and c_{θ_2} taking respectively the values 3.0 and 0.5. When expressions (18) and (19) have been considered the values retained for the coefficients c_{θ_1} and c_{θ_1}' are those proposed by Samaraweera [17], 4.3 and −3.2 respectively.

Three different approximated schemes have been tested for the diffusion terms $D(\overline{u_j\theta})$ which at high turbulent Reynolds and Peclet numbers associated with the hypothesis $\overline{p\theta}/\rho = 0$ reduced to

$$-\frac{\partial}{\partial x_k}(\overline{u_j u_k\theta}).$$

—The simpler version proposed by Wyngaard and Cote [18]

$$D(u_j\theta) = \frac{\partial}{\partial x_k}\left(0.15\frac{k}{\varepsilon}\overline{u_k u_l}\frac{\partial \overline{u_j\theta}}{\partial x_l}\right), \text{ model } R_{T_4}. \quad (21)$$

—The version adopted by Launder [12]

$$D(\overline{u_j\theta}) = \frac{\partial}{\partial x_k}\left[c_\theta\frac{k}{\varepsilon}\left(\overline{u_k u_l}\frac{\partial \overline{u_j\theta}}{\partial x_l} + \overline{u_j u_l}\frac{\partial \overline{u_k\theta}}{\partial x_l}\right)\right], \text{ model } R_{T_2} \quad (22)$$

the coefficient c_θ been taken, by analogy with the stress-diffusion model, as 0.11.

—The version adopted by Dekeyser [2]

$$D(\overline{u_j\theta}) = \frac{\partial}{\partial x_k}\left[\hat{c}_\theta\frac{k}{\varepsilon}\left(\overline{u_k u_l}\frac{\partial \overline{u_j\theta}}{\partial x_l} + \overline{u_j u_l}\frac{\partial \overline{u_k\theta}}{\partial x_l} + \overline{u_l\theta}\frac{\partial \overline{u_j u_k}}{\partial x_l}\right)\right], \text{ models } R_{T_1}, R_{T_3} \quad (23)$$

the coefficient $\hat{c}_\theta$ taking the optimized value 0.15.

Closure of the thermal field is completed through the following equation governing the transport of the mean square temperature fluctuations

$$U_k \frac{\partial}{\partial x_k}\left(\frac{\overline{\theta^2}}{2}\right) = P_\theta - \varepsilon_\theta + D\left(\frac{\overline{\theta^2}}{2}\right). \tag{24}$$

The three terms appearing in the right side of equation (24) express how the level of $\overline{\theta^2}$ will change through: the generative action of mean temperature gradients

$$P_\theta = -\overline{u_j\theta}\frac{\partial \Theta}{\partial x_j}$$

(which requires no approximation); the dissipation due to molecular diffusion in the fine scale motions; and the diffusive transport produced by turbulent velocity fluctuations and molecular dispersion

$$D\left(\frac{\overline{\theta^2}}{2}\right) = -\frac{\partial}{\partial x_j}\left[\frac{\overline{u_j\theta^2}}{2} - \alpha\frac{\partial}{\partial x_j}\left(\frac{\overline{\theta^2}}{2}\right)\right].$$

At high turbulent Reynolds numbers and for fluids with Prandtl numbers not too small the diffusive transport of $\overline{\theta^2}/2$ reduced to

$$-\frac{\partial}{\partial x_j}\left(\frac{\overline{u_j\theta^2}}{2}\right).$$

Two models have been considered here. The first proposal which is in common use[17, 19], consisting of a simple gradient type representation for the triple velocity–temperature correlation

$$D\left(\frac{\overline{\theta^2}}{2}\right) = \frac{\partial}{\partial x_k}\left[c_g\frac{k}{\varepsilon}\overline{u_k u_l}\frac{\partial}{\partial x_l}\left(\frac{\overline{\theta^2}}{2}\right)\right],$$

models $R_{T_1}, R_{T_2}, R_{T_3}$ (25)

and the version adopted by Deardorff [20] and Wyngaard and Cote [18]

$$D\left(\frac{\overline{\theta^2}}{2}\right) = \frac{\partial}{\partial x_k}\left[c_g\frac{k}{\varepsilon}\left(\overline{u_k u_l}\frac{\partial}{\partial x_l}\left(\frac{\overline{\theta^2}}{2}\right) + \overline{u_l\theta}\frac{\partial \overline{u_k\theta}}{\partial x_l}\right)\right],$$

model R_{T_4}. (26)

By analogy with the stress-diffusion model c_g has been chosen as 0.11.

The more important term needing approximation in equation (24) is the dissipation rate of $\overline{\theta^2}/2$. So far, the published modelled forms of transport equation for ε_θ being at best tentative, we have expressed this by definition of the time scale ratio R as

$$\varepsilon_\theta = \frac{1}{R}\frac{\varepsilon}{k}\frac{\overline{\theta^2}}{2}. \tag{27}$$

The results available in the literature shows that the ratio R is not a constant. In thin shear flows the proposed values [17, 19, 21, 22, 23] show a wide range between 0.5 and 0.8. The experimental programme carried out to examine the asymmetrical heated plane jet [2] has shown a substantial variation of R across the stream but notwithstanding we have chosen a constant value of about 0.65 which is about the average level indicated. It will be seen later that this choice gives good agreement between computed and measured levels of the mean square temperature fluctuations.

3. SOLUTION OF EQUATIONS

Use of the model of turbulence described in section 2 for heat transfer in two-dimensional thin shear flows like the heated asymmetrical plane jet requires solution of transport equations for the Reynolds stresses $\overline{u_1^2}$, $\overline{u_2^2}$, $\overline{u_3^2}$ and $\overline{u_1u_2}$ (x_1 denoting the streamwise direction and x_2 the direction of principal gradient of velocity and temperature), for the energy dissipation rate ε, for the turbulent heat fluxes $\overline{u_1\theta}$ and $\overline{u_2\theta}$, for the mean square temperature fluctuations $\overline{\theta^2}$, in addition to the dependent variables for the mean field. Moreover, though this is not a necessity the turbulence kinetic energy is calculated according to its own modelled transport equation.

In the diffusive terms on the right-hand sides of the transport equations for turbulence variables only the cross-stream component is of significance for thin shear flows. The resulting set of modelled equations is parabolic and the widely known finite-difference method of Patankar and Spalding [24] can be used as basis for the numerical solution. The original procedure was formulated for use with an effective viscosity and an effective diffusivity scheme for modelling diffusive transport. So a number of modifications to the basic structure had to be introduced. The most important of these consists, following Andre *et al.* [25], Pope and Whitelaw [26] and Samaraweera [17], to stagger the location of nodes for the turbulence variables relative to mean-field nodes. Typically 41 nodes across the flow were used. The initial conditions have been deduced from the measurements of the velocity and temperature fields at the exit of the slot (section $x_1/d = 0$) [2].

4. PRESENTATION AND DISCUSSION OF RESULTS

A definition sketch of the flow showing the initial and fully developed mean velocity and temperature profiles is given in Fig. 1.

4.1. *Velocity field*

Comparisons between experimental results and numerical prediction have been made with two models R_{D_1} and R_{D_2} only different in the modelling adopted for the diffusive transport of stress $D(\overline{u_iu_j})$.

Figure 2 shows a relatively close agreement for the decay of the maximum velocity in the streamwise direction. The differences between experiment and calculations in the initial part of the flow may be due either to the hypothesis of thin shear flow or to the uncertainties in the initial conditions concerning the

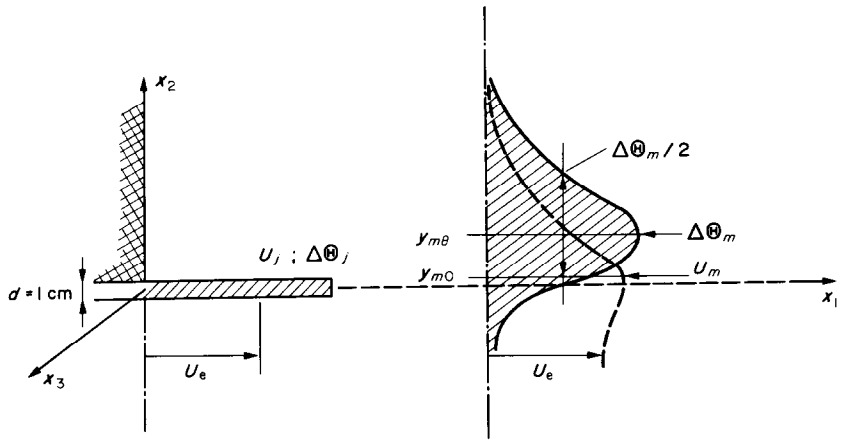

FIG. 1. Definition sketch of the flow.

levels of k and ε in the turbulent boundary layers in the experimental apparatus upstream the exit slot.

Figure 2 shows also a good agreement for the spreading represented by the velocity length scale $l_{u_1} = (x_{2_i} - x_{2_e})/2$ where x_{2_i} is the streamwise position corresponding to the mean velocity level $(U_m + U_i)/2$ situated on the low velocity side ($U_i = 0$) and x_{2_e} corresponding to the mean velocity level $(U_m + U_e)/2$ situated on the high velocity side of the flow.

The calculated mean velocity distributions obtained with R_{D_1} and R_{D_2} are compared to the experimental data, in Fig. 3, at downstream section $x_1/d = 50$. The agreement is very satisfactory for R_{D_2}. Concerning R_{D_1} a shift towards the low velocity side can be observed. It appears (Fig. 2) that R_{D_1}, which uses a simple gradient-type representation for the diffusive transport of stress, gives a good rate of growth of the flow but gives a too rapid expansion on the low velocity side and a too slow rate on the high velocity side.

The distributions of the normal stresses $\overline{u_1^2}, \overline{u_2^2}, \overline{u_3^2}$ and the turbulent kinetic energy k shown in Fig. 4 display a generally close agreement with measurements, the maximum values are correctly predicted, though we notice that the calculated values fall to zero more rapidly than the measurements towards the high velocity edge and less rapidly toward the low velocity side. We thus observe shift of the calculated turbulent field towards the low velocity side of the order of 15–20% of the width of the flow. Similar results have been obtained by Hanjalic and Launder [7], Schiestel [27] and Samaraweera [17] in predicting the mixing layer generated between a moving stream and a stationary field.

The turbulent energy distributions $\overline{u_i^2}/k$ are shown in Fig. 5. It can be observed that both numerical and experimental investigations give

$$\frac{\overline{u_1^2}}{k} \sim 1; \quad \frac{\overline{u_2^2}}{k} \sim 0.5; \quad \frac{\overline{u_3^2}}{k} \sim 0.5,$$

although the calculated behaviour of the energy

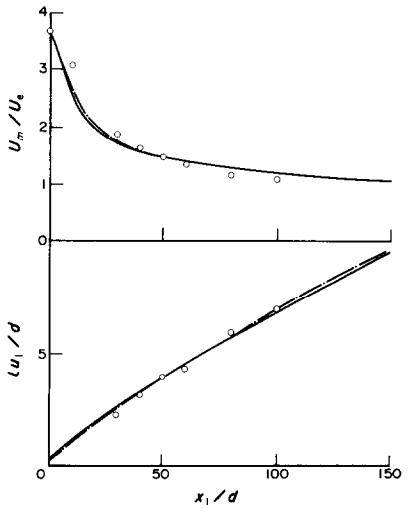

FIG. 2. Variations of mean velocity intensity and velocity length scale; ○ data of Dekeyser [2]; —·— model R_{D_1}; —— model R_{D_2}.

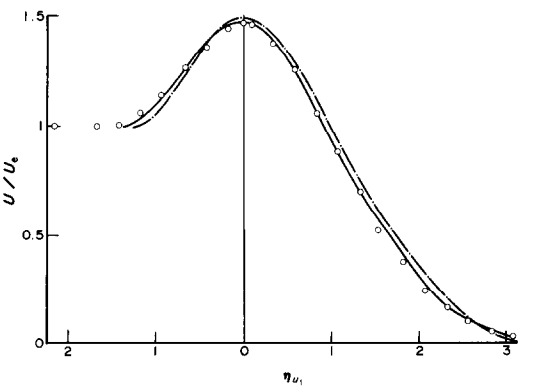

FIG. 3. Mean velocity profile; for legend see Fig. 2.

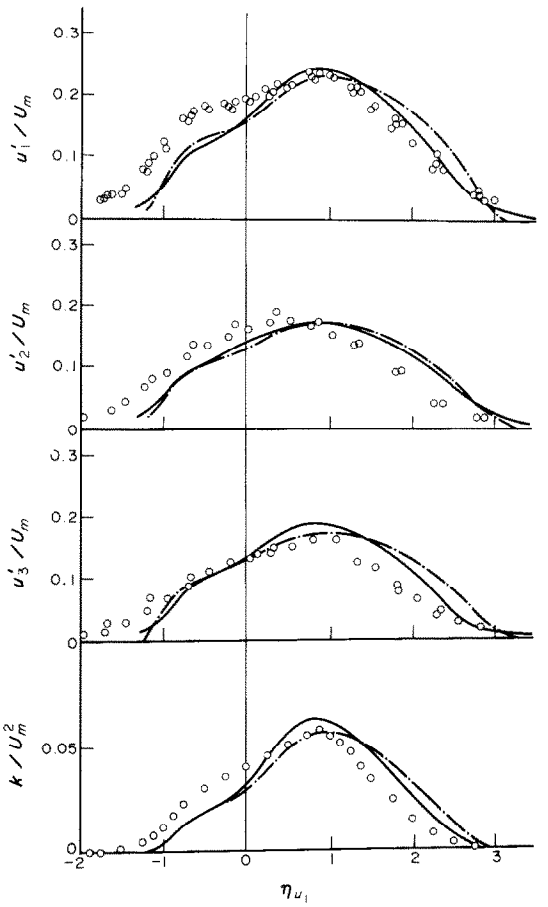

FIG. 4. Profiles of velocity fluctuations intensity and kinetic energy; for legend see Fig. 2.

distributions are not in agreement with experimental data

$$\frac{\overline{u_1^2}}{k} > \frac{\overline{u_2^2}}{k} \geqslant \frac{\overline{u_3^2}}{k}.$$

This can be attributed to the thin shear layer hypothesis

$$\left(\frac{\partial}{\partial x_1} \ll \frac{\partial}{\partial x_2}\right)$$

since the normal stresses are sensitive to the production terms resulting from the $\partial/\partial x_1$ gradients [11]. It should also be noted that the behaviours of models R_{D_1} and R_{D_2} are different at the edges of the flow.

The calculated profiles of the Reynolds shear stress $\overline{u_1 u_2}$ shown in Fig. 6 are in close agreement with the experimental data. The experimental observed displacement occurring between the points where the viscous and turbulent shear stresses are zero is satisfactorily predicted by R_{D_2} and somewhat less satisfactorily by R_{D_1}. It is of interest to consider the correlation $R_{u_1 u_2}$. The predicted distributions shown in Fig. 6 display close agreement with measurement in the centre of the flow. At the edges the behaviours of the calculated correlations are not satisfactory: R_{D_1} falls

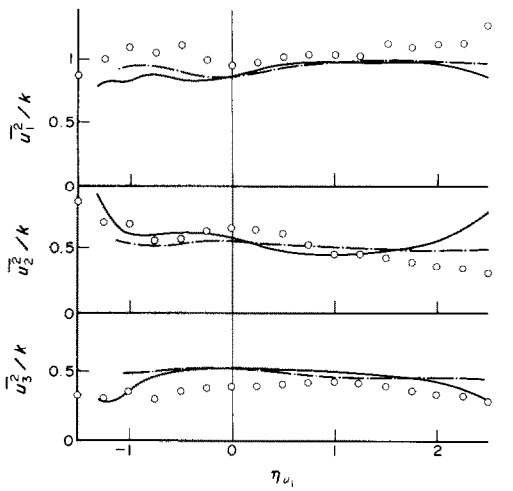

FIG. 5. Turbulence energy distribution; for legend see Fig. 2.

abruptly to zero while R_{D_2} grows equally abruptly before going to zero. Similar results have been reported previously by [17]. It can be observed that these anomalies occurs in regions of the flow concerning small values of the turbulent shear stress so that their influence on the numerical predicting can be considered to be negligible.

The term representing the production of turbulent kinetic energy $\pi_1 = -(\overline{u_1 u_2})\,\partial U_1/\partial x_2$ is shown in Fig. 7. The numerical distributions display close agreement with measurement in particular the region of negative values of π_1 and also the two peaks of π_1 are correctly predicted although the predicted values of the peak of production situated on the low velocity edge are somewhat too high.

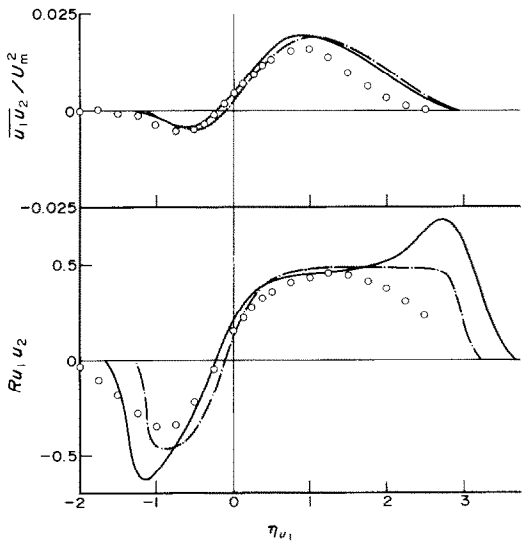

FIG. 6. Shear stress profiles and shear correlation coefficient; for legend see Fig. 2.

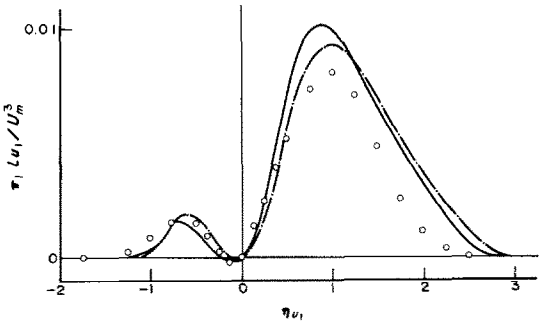

FIG. 7. Production of turbulent kinetic energy; for legend see Fig. 2.

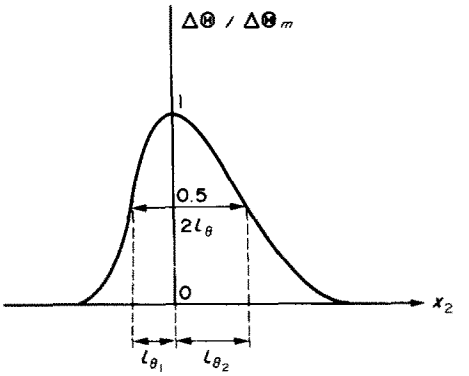

FIG. 9. Definition sketch of temperature length scales l_{θ_1} and l_{θ_2}.

4.2. *Temperature field*

The decay of the mean thermal intensity scale $\Delta\Theta_m/\Delta\Theta_{m0}$ predicted from models $R_{D_2}-R_{T_1}$, $R_{D_2}-R_{T_3}$ and $R_{D_1}-R_{T_2}$ are indistinguishable. The agreement of predictions with measured evolution is not satisfactory particularly in the initial part of the flow (Fig. 8) although the predicted level at section $x_1/d = 50$ agrees well with the measured level. Figure 8 shows also the variation of length scale for the temperature field l_θ/d; $2l_\theta$ being the distance between the half maximum intensity of the temperature profile. The predictions from models $R_{D_2}-R_{T_3}$ and $R_{D_2}-R_{T_1}$ are virtually the same. The agreement of predictions with measurement is within 10%.

The mean temperature profiles are markedly asymmetric, the steeper gradient occurring on the high velocity side. For this reason the following profiles for the thermal field will be scaled by l_{θ_1} for the high velocity side and l_{θ_2} for the low velocity side according to the definition sketch in Fig. 9; thus the non-dimensional length scales

$$\eta_{\theta_i} = \frac{x_2 - x_{2\Delta\Theta_m}}{l_{\theta_i}}$$

will be considered.

At section $x_1/d = 50$ the predicted mean temperature profiles compare very satisfactory with the experimental data (Fig. 10). Near the free stream the agreement of the predictions by model $R_{D_1}-R_{T_2}$ with measurements deteriorates, the predictions show a more abrupt approach to free stream conditions than do the measurements.

The predicted level of the peak of temperature fluctuation intensity situated near the moving edge by model $R_{D_1}-R_{T_2}$ is about 20% too high compared with the measured level (Fig. 11). The predictions by models $R_{D_2}-R_{T_1}$ and $R_{D_2}-R_{T_3}$ are in excellent agreement with the experimental data particularly in the centre of the flow, the agreement is within 5% at the edges of the flow.

Figure 12 shows that the agreement for the cross-stream heat flux $\overline{u_2\theta}$ is less satisfactory. As can be seen the experimentally observed separation between the points where the turbulent cross-stream heat flux and the mean temperature gradient are zero is not correctly

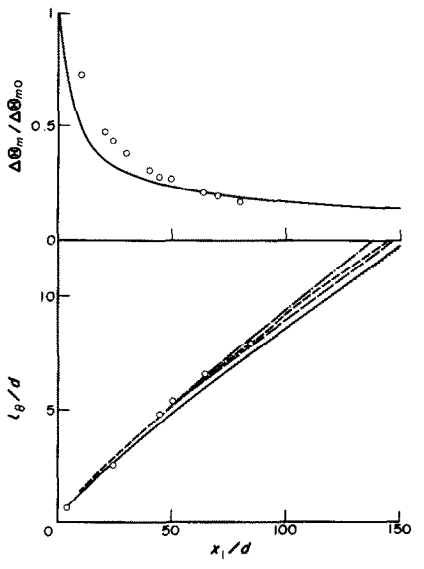

FIG. 8. Variations of mean temperature intensity and temperature length scales (l_θ/d); ○ data of Dekeyser [2]; —— model $R_{D_2}-R_{T_1}$; --- model $R_{D_2}-R_{T_2}$; ···· model $R_{D_2}-R_{T_3}$; — — model $R_{D_2}-R_{T_7}$; —·— model $R_{D_1}-R_{T_2}$.

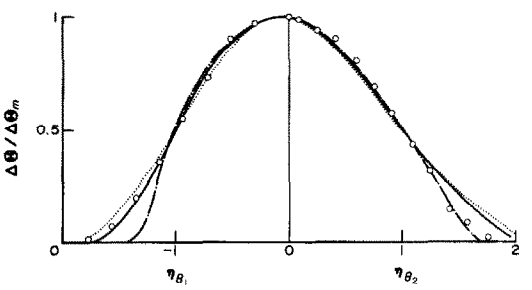

FIG. 10. Mean temperature profile; ○ data of Dekeyser [2]; —— model $R_{D_2}-R_{T_1}$; ···· model $R_{D_2}-R_{T_3}$; —·— model $R_{D_1}-R_{T_2}$.

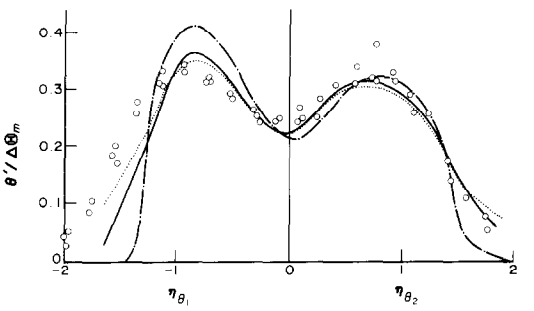

FIG. 11. Profile of temperature fluctuation intensity; for legend see Fig. 10.

predicted particularly by model $R_{D_1}-R_{T_2}$ which uses the simple gradient versions for modelling the triple correlations.

It is of interest to compare (Table 1) the different experimental and predicted displacements arising in the heated asymmetrical plane jet. It can be noted that both numerical and experimental date indicate that:

$$x_{2_{\Delta\Theta_m}} > x_{2_{\overline{u_2\theta}=0}} > x_{2U_m} > x_{2_{\overline{u_1u_2}=0}}$$

though the predicted displacement of the mean temperature field towards the mean velocity field is too low.

There is (Fig. 12) a considerable difference between the predicted and measured levels of the streamwise heat flux $\overline{u_1\theta}$ near the moving edge of the flow, the predictions being consistently lower than the measurements, about 45% for model $R_{D_2}-R_{T_1}$ and 65% for models $R_{D_2}-R_{T_1}$ and $R_{D_2}-R_{T_3}$. It is acknowledged that the streamwise heat flux is highly influenced by the contribution of the pressure-temperature correlation; also it is paradoxical to observe that the models $R_{D_2}-R_{T_1}$ and $R_{D_2}-R_{T_3}$ which compare two different closure schemes for this term, should give approximately the same results. The level predicted by model $R_{D_2}-R_{T_1}$ is in accordance with the under-estimate of the level of the temperature fluctuation intensity predicted by this model in the same region of the flow.

Figure 13 shows the predicted correlations $R_{u_1\theta}$ and $R_{u_2\theta}$ compared with the experimental data. Concerning $R_{u_1\theta}$ there is a large discrepancy between predictions and measurements. The predicted levels of $R_{u_2\theta}$ are, in the centre of the flow, in satisfactory agreement with the

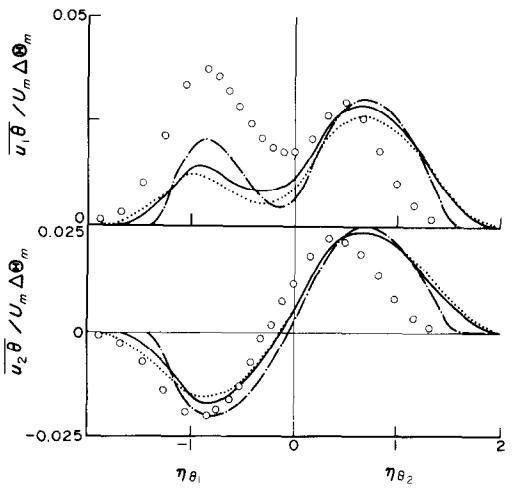

FIG. 12. Streamwise and cross-stream heat fluxes; for legend see Fig. 10.

experimental data while at the edges of the flow the same effect that was seen in the shear correlation coefficient can be observed.

The numerical predictions of the production of temperature fluctuation intensity $\pi_{1\theta} = (\overline{u_2\theta})\,\partial\Theta/\partial x_2$ show a satisfactory agreement with the experimental

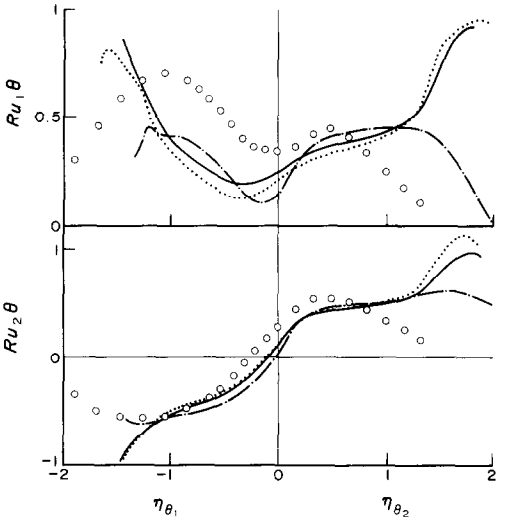

FIG. 13. Temperature correlations: for legend see Fig. 10.

Table 1

	$x_{2\Delta\Theta_m}-x_{2U_m}$	$x_{2U_m}-x_{2\overline{u_1u_2}=0}$	$x_{2\Delta\Theta_m}-x_{2\overline{u_2\theta}=0}$	$x_{2\overline{u_2\theta}=0}-x_{2U_m}$
Experiment	2	0.8	1.3	0.7
Model $R_{D_2}-R_{T_1}$	0.89	0.9	0.55	0.34
Model $R_{D_2}-R_{T_3}$	0.72	0.9	0.48	0.24
Model $R_{D_1}-R_{T_2}$	0.94	0.43	0.1	0.84

All values are in cm.

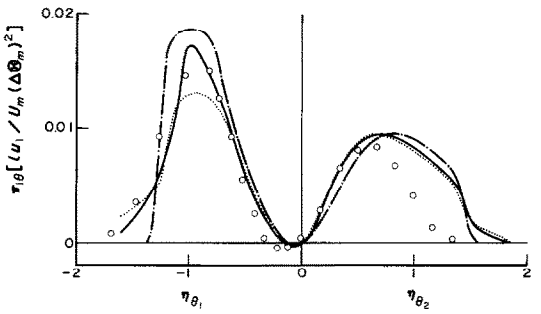

FIG. 14. Production of temperature fluctuation intensity; for legend see Fig. 10.

data (Fig. 14) particularly for model $R_{D_2}-R_{T_1}$. So the existence of negative values is well predicted, but consistently with the previous results, a shift of these negative zones towards the lower velocity side of the flow can be observed.

5. CONCLUDING REMARKS

The previous section has considered the prediction of heat transport in a heated asymmetrical plane jet. Generally the different models used for the prediction have achieved a satisfactory level of agreement, particularly model $R_{D_2}-R_{T_1}$.

Except for the level of the streamwise heat flux on the high velocity side of the flow, no notable differences have emerged in the comparison of calculation with experiment. It has been noted that the two different closure schemes for the pressure–temperature gradient correlation give quite similar results for the levels of $\overline{u_1\theta}$. This suggests that the defect in predicting the correct level of $\overline{u_1\theta}$ may originate in the time-scale used for the modelling of $\phi_{i\theta}^{(1)}$ which is a sink term in the $\overline{u_i\theta}$ equations. A timescale properly characteristic of the fluctuating temperature field like $\overline{\theta^2}/2\varepsilon_\theta$ has not been considered in the present work; instead this quantity has been assumed proportional to k/ε which is entirely unaffected by the temperature field. So to handle flows of the present type the provision of a transport equation for ε_θ seems appropriate.

In the prediction of plane wakes and mixing layers with a stagnant stream [16], defects in predicting the temperature field often spring principally from shortcomings in the hydrodynamic model. Improvements in the modelling of the pressure interaction and diffusion processes would be of interest.

Acknowledgements—The author gratefully acknowledges the help of Dr D. S. A. Samaraweera who made the major adaptations of the computer program used in this work. He also thanks Professor B. E. Launder for his support and helpful suggestions.

REFERENCES

1. J. C. Rotta, Statistische theorie nichthomogener turbulenz, *Z. Phys.* **129,** 547–572, **131,** 51–77 (1951).
2. I. Dekeyser, Etude d'un jet plan dissymétrique chauffé en régime turbulent incompressible, Thèse de Doctorat d'Etat, Université d'Aix-Marseille II (1982).
3. A. Favre, Equations des gaz turbulents compressibles, I—Formes générales, *J. Méc.* **4,** 361–390 (1965) and II—Méthode des vitesses moyennes; méthode des vitesses macroscopiques pondérées par la masse volumique, *J. Méc.* **4,** 390–421 (1965).
4. D. Naot, A. Shavit and M. Wolfshstein, Interaction between components of the turbulence velocity correlation tensor, *Israel J. Tech.* **8,** 259 (1970).
5. M. M. Gibson and B. E. Launder, Ground effects on pressure fluctuations in the atmospheric boundary layer, *J. Fluid Mech.* **86,** 491–511 (1978).
6. M. M. Gibson and W. Rodi, A Reynolds stress closure model of turbulence applied to the calculation of a highly curved mixing layer, *J. Fluid Mech.* **103,** 161–182 (1981).
7. K. Hanjalic and B. E. Launder, A Reynolds stress model of turbulence and its application to thin shear flows, *J. Fluid Mech.* **52,** 609–638 (1972).
8. B. J. Daly and F. H. Harlow, Transport equations in turbulence, *Phys. Fluids* **13,** 2634–2649 (1970).
9. A. Morse, Axisymmetric turbulent shear flows with and without swirl, Ph. D. Thesis, University of London (1980).
10. B. E. Launder, G. J. Reece and W. Rodi, Progress in the development of a Reynolds stress turbulence closure, *J. Fluid Mech.* **68,** 537–566 (1975).
11. B. E. Launder and A. Morse, Numerical prediction of axisymmetric free shear flow with a second-order Reynolds stress closure. *Proc. 1st Symposium on Turbulent Shear Flow*, Penn. State Univ., U.S.A. (1977). *Lecture Notes in Physics.* Springer Verlag (1979).
12. B. E. Launder, Heat and mass transport in turbulence, in *Topics in Applied Physics*, vol. 12 (edited by P. Bradshaw). Springer, Berlin (1976).
13. A. S. Monin, On the symmetry properties of turbulence in the surface layer of air, *Izv. Atmos. Oceanic Phys.* **1,** 45 (1965).
14. J. L. Lumley and B. Khajeh-Nouri, Computational modeling of turbulent transport, *Adv. Geophys.* **18A,** 169–192 (1974).
15. B. E. Launder, Scalar property transport by turbulence, Rep. No. HTS/73/26 Dept. Mech. Eng., Imperial College, London (1973).
16. B. E. Launder and D. S. A. Samaraweera, Application of a second-moment turbulence closure to heat and mass transport in thin shear flows. I—Two-dimensional transport, *Int. J. Heat Mass Transfer* **22,** 1631–1643 (1979).
17. D. S. A. Samaraweera, Turbulent heat transport in two- and three-dimensional temperature fields, Ph. D. Thesis, Faculty of Engineering, University of London (1978).
18. J. C. Wyngaard and O. R. Cote, The evolution of a convective planetary boundary layer. A higher order closure model study, *Boundary Layer Meteorol.* **7,** 289–308 (1974).
19. J. C. Wyngaard, Modeling the planetary boundary layer. Extension to the stable case, *Boundary Layer Meteorol.* **9,** 441–460 (1975).
20. J. W. Deardorff, Three dimensional numerical modeling of the planetary boundary layer, Workshop on micrometeorology, *Am. Meteorol. Soc.*, 271–311 (1973).
21. D. B. Spalding, Concentration fluctuations in a round turbulent free jet, *Chem. Engng Sc.* **62,** 95 (1975).
22. B. E. Launder, On the effects of a gravitational field on the turbulent transport of heat and momentum, *J. Fluid Mech.* **67,** 569–581 (1975).
23. C. Beguier, I. Dekeyser and B. E. Launder, Ratio of scalar and velocity dissipation time scales in shear flow turbulence, *Phys. Fluids* **21,** 307–310 (1978).
24. S. V. Patankar and D. B. Spalding, *Heat and Mass Transfer in Boundary Layers*, 2nd edn. Intertex Books, London (1970).
25. J. C. Andre, G. De Moor, P. La Carrere and R. Du Vachat,

Turbulence approximation for inhomogeneous flows: part II. The numerical simulation of a penetrative convection experiment, *J.A.S.* **33,** 482–491 (1976).
26. S. B. Pope and J. H. Whitelaw, The calculation of near-wake flows, *J. Fluid Mech.* **73,** 9–32 (1976).
27. R. Schiestei Sur un nouveau modèle de turbulence appliqué aux transferts de quantité de mouvement et de chaleur, Thèse de Doctorat d'Etat, Université de Nancy I (1974).

PREDETERMINATION NUMERIQUE A L'AIDE D'UNE FERMETURE AU SECOND ORDRE D'UN JET PLAN DISSYMETRIQUE CHAUFFE

Résumé—Le présent article a pour objet le calcul d'un jet plan dissymétrique chauffé en régime turbulent incompressible en faisant appel à des schémas de fermeture locaux au second ordre. Différentes modélisations des corrélations triples de vitesse et de vitesse–température ont été testées. Les résultats numériques obtenus à l'aide d'une méthode aux différences finies déduite de celle de Patankar–Spalding, la principale modification consistant en l'utilisation, pour la localisation des variables turbulentes, d'une maille de discrétisation décalée à partir de la maille conventionnelle, ont été comparés aux résultats expérimentaux.

NUMERISCHE BERECHNUNG EINES ASYMMETRISCH BEHEIZTEN EBENEN STRAHLS MIT EINEM TURBULENZMODELL ZWEITER ORDNUNG

Zusammenfassung—Dieser Bericht befaßt sich mit der Berechnung eines asymmetrisch beheizten ebenen Strahls unter Anwendung eines Turbulenzmodells zweiter Ordnung. Unterschiedliche Ansätze für räumliche Geschwindigkeitsverteilung und Geschwindigkeits-Temperatur-Korrelationen wurden untersucht. Die Rechenergebnisse, die mit einem modifizierten Patankar–Spalding-Differenzenverfahren erhalten wurden, bei dem die wichtigsten Modifikationen die Veränderung der Lage der Knoten für die Turbulenzvariablen zu den Feldknoten waren, werden mit experimentellen Daten verglichen.

ЧИСЛЕННЫЙ РАСЧЕТ АСИММЕТРИЧНО НАГРЕТОЙ ПЛОСКОЙ ТУРБУЛЕНТНОЙ СТРУИ НА ОСНОВЕ МОДЕЛИ ВТОРОГО ПОРЯДКА

Аннотация—В работе модель второго порядка использована для расчета асимметрично нагретой плоской струи. Исследованы различные варианты аппроксимации тройных корреляций скорости и корреляций скорость-температура. Численные решения, полученные с помощью модифицированного конечно-разностного метода Патанкара-Сполдинга (наиболее важная особенность модификации-совмещение узлов турбулентного поля с узлами среднего поля), сравниваются с экспериментальными данными.